JOURNAL OF MATERIALS SCIENCE 24 (1989) 681–687

Fracture surface roughness as a gauge of fracture toughness: aluminium–particulate SiC composites

D. L. DAVIDSON
Southwest Research Institute, 6220 Culebra Road, San Antonio, Texas 78284, USA

Fracture toughnesses of several composites of aluminium alloys reinforced with particulate SiC have been measured. The variables were particulate size and volume fraction, and matrix alloy composition and heat treatment. Fracture surface profiles were measured and related to fractal dimension using the techniques of quantitative metallography. The fracture surface roughness was described well by fractals, but fracture toughness did not correlate with any measure of fracture surface roughness. An explanation for this behaviour is offered.

1. Introduction

Fracture toughness is a measurement of the work done during fracture. If microstructure of the material increases the roughness of the fracture surface, then the work done during fracture should be increased because of the increase in newly created surface area. This conjecture follows directly from the Griffith relationship between surface energy γ, stress σ and crack length a. The Griffith relationship is strictly true only for brittle materials. For more ductile solids, γ should be considered as being the energy expended per unit area of crack surface increase, which would include the contribution of a plastic zone surrounding the growing crack.

$$K_c = \sigma^{1/2} a = 2E\gamma \quad (1)$$

It is not easy to examine the relationship between fracture surface roughness and fracture toughness because of the difficulty in measuring surface roughness. Quantitative fractography methods have been developed for this purpose [1], but they are seldom applied because difficult and time-consuming measurements are required. In addition, some of the quantitative methods developed for determining roughness have not been extensively tested. Fractal geometry has been recently suggested as a suitable model for fracture surface roughness [2, 3], but this hypothesis is still being examined.

The purposes of the present paper are to (i) report on measurements of fracture surface roughness and (ii) relate these to fracture toughness values measured from the same materials. This work was done as a by-product of studying the influence of manufacturing and processing variables on the fracture toughness of aluminium alloys reinforced with particulate silicon carbide.

2. Experimental procedure

This section describes the materials tested, how fracture toughness values were determined, and the method used to measure the roughness of the fast fracture surfaces.

2.1. Materials

Aluminium alloys reinforced with 15 and 25 vol % particulate silicon carbide were manufactured by two methods:

1. Mechanical alloying (MA) was used by Novamet (Huntington, West Virginia) to make both alloying additions and to mix in the silicon carbide particulate. The high-energy ball-milling used for alloying resulted in powders which were then consolidated, sintered, and finally extruded.
2. Conventional ingot methods (IM) were used by Dural Aluminum Composite Co. (San Diego, California) to cast billets of composite which were then hot-extruded.

The materials made by these two methods are listed in Table I. Alloys which could be hardened by precipitation-ageing treatments were tested in the as-received (extruded) and peak-aged conditions. Time–temperature treatments for peak ageing were supplied by the manufacturers and were not independently verified.

2.2. Fracture toughness

Compact-tension specimens of the dimensions shown in Fig. 1 were tested. After heat treatment, specimen blanks were machined to finished dimensions. These specimens were then further polished using metallurgical specimen preparation techniques.

Fatigue cracks were initiated from the notch at $\Delta K \leqslant 8\,\mathrm{MPa\,m^{1/2}}$. All testing was done in a computer-controlled fatigue machine and crack length was measured by compliance. Load was shed as the fatigue cracks grew until a rate of about 10^{-10} m per cycle was reached. The load was then slightly increased and the fatigue crack was grown until the specimen broke. The fracture toughness, K_c, was determined from the

0022–2461/89 $03.00 + .12

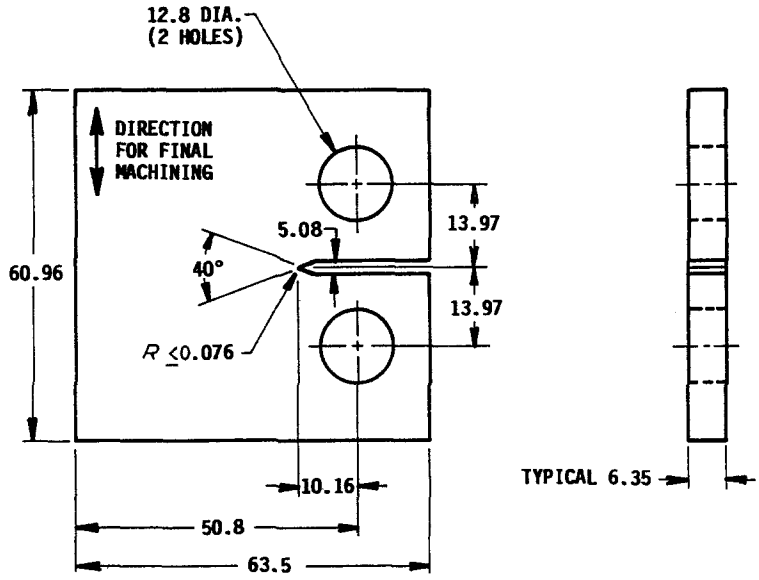

Figure 1 Design and dimensions (mm) of the specimens used for the measurement of fracture toughness.

geometry of the specimen and the final load and crack length at the onset of fast fracture. The fatigue and fast-fracture regions were distinct, enabling the crack length at final fracture to be easily verified by manual measurement.

By the testing method described above, it was possible to obtain both fatigue crack growth and fracture toughness data. Values of fracture toughness obtained by this method, although not matching the ASTM standard, are considered to be valid, reliable, and representative of the material. The conditions used in testing are reasonably representative of a failure which might occur during actual usage. Duplicate specimens were tested for most of the materials in order to determine the reproducibility of the values measured.

2.3. Fracture surface roughness

One fracture surface of each material was lightly plated with electroless nickel and then mounted in a metallurgical mount and sectioned both parallel and perpendicular to the direction of crack growth. Optical photographs were made from these cross-sectional views at several magnifications. For further analysis, 200 × proved to be the appropriate enlargement, as will be further discussed later.

Software for a Dapple image analysis system was modified to recognize the fracture surface, which allowed the 108 mm of photograph width to be broken into 254 pixels. Having a coordinate position for each pixel along the fracture surface allowed the length of the profile to be computed. At 200 × the surface location was, therefore, specified each 2.12 μm, and in multiples thereof.

The length of a fracture surface profile is dependent upon the spatial acuity used in making the measurement [4]. In other words, for a fixed measuring unit size, the profile length measured depends on the magnification used to view the profile. Computationally, it is easier to vary the measuring unit size η than the photograph magnification. The variation in profile length with η is then used to determine the "true" profile length; for this case, $\eta = 2.12\,\mu$m and multiples of this value. The surface profile length was used to compute the profile roughness parameter, defined [3] as

$$R_L = \frac{\text{Actual profile length}}{\text{Projected profile length}}$$

It will be shown that R_L is η-dependent, and that a value, $R_L(0)$, can be determined which is the reference roughness parameter. From $R_L(0)$, the surface roughness parameter R_S, similar in definition to R_L, but for surfaces, is determined [3] using the relation

$$R_S = \frac{4}{\pi}(R_L - 1) + 1 \qquad (2)$$

If the hypothesis posed in the introduction is correct, then as R_S increases, so should K_c.

TABLE I Materials examined

Process type*	Matrix alloy	Volume fraction SiC (%)	Age-hardening alloy?
MA	IN-9052	15	No
IM	Al-4Mg	15	No
MA	IN-9021	14	Yes
IM	2014	15	Yes
IM	2014	25	Yes
IM	2024	15	Yes
IM	7475	15	Yes

*MA = mechanically alloyed, IM = ingot metallurgy.

3. Results

The results of the fracture surface roughness measurements will first be examined in some detail, then the values of surface roughness parameter will be compared with measured fracture toughnesses.

3.1. Fracture surface roughness

Some examples of cross-sectional views through fast fracture zones of the fracture toughness specimens are shown in Fig. 2. The mechanically alloyed material clearly has a much finer average size of SiC than that made by casting. Also the distribution of SiC is more uniform in the mechanically alloyed material.

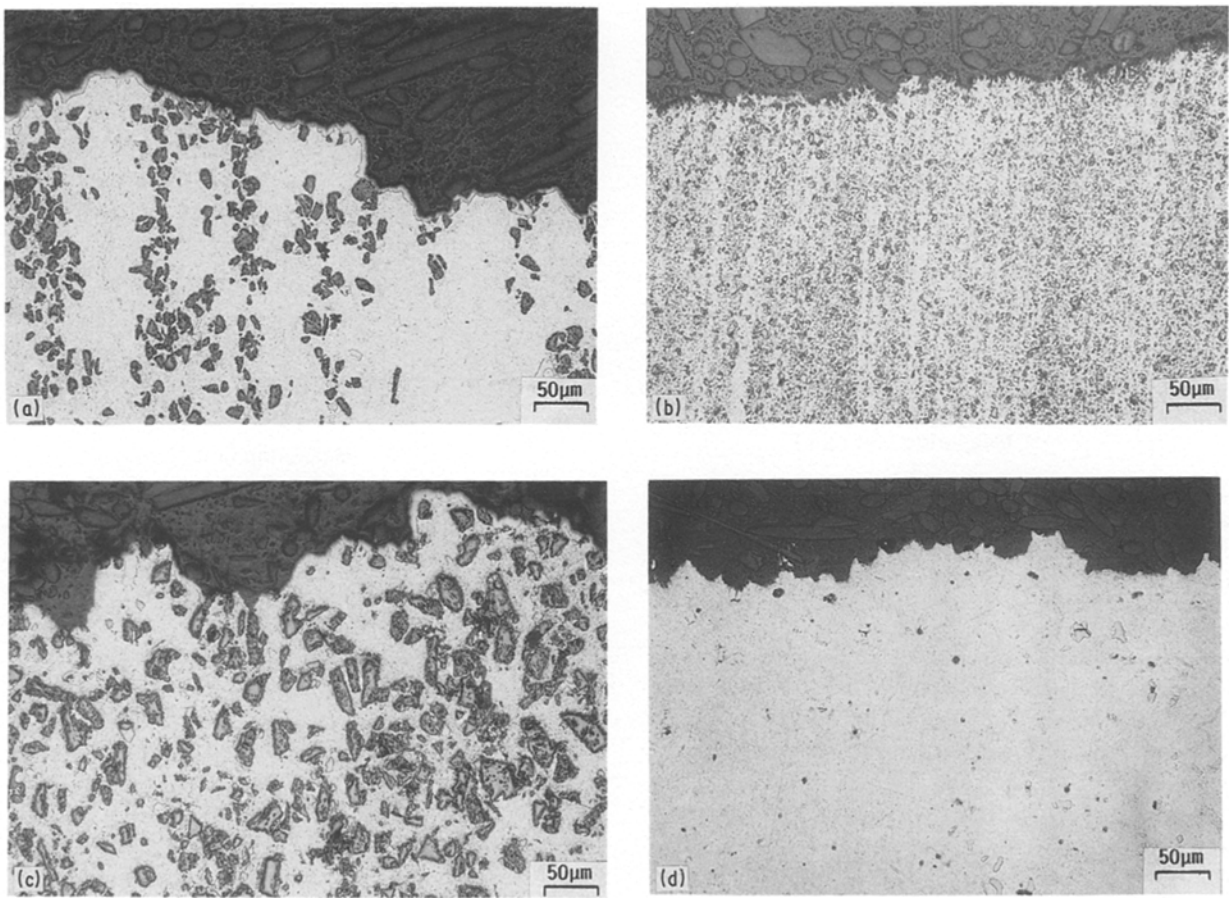

Figure 2 Examples of fast-fracture surface profiles from which roughness values were measured. Crack growth direction was left to right. The differences in SiC size and distribution are obvious, but the similarity in surface roughness between (a) and (b) is not (see Tables III and V). (a) Alloy 6, $R_S(0) = 2.26$; (b) Alloy 4, $R_S(0) = 2.34$; (c) Alloy 8, $R_S(0) = 2.8$; (d) Alloy 12, $R_S = 1.69$.

Increasing the volume fraction of SiC increases the uniformity of distribution (Fig. 2c).

Once surface profiles of the fast-fracture region were digitized from photographs such as those shown in Fig. 2, the image processing system determined values of the roughness parameter R_L with increasing values of the measuring unit (η). From these values of R_L, Equation 2 was used to compute R_S. Resulting roughness values for the fracture surfaces shown in Fig. 2 are given in Table II.

According to some previous measurements of surface roughness [1, 2, 5], these parameters may have a linear relationship when plotted as $\log R_L$ against $\log\eta$. The same would be true for $\log R_S$ against $\log\eta$. This relationship was examined for R_S, but so were several others; these are given as Equations 3 to 6 in Table III, together with the values of the parameters derived from the surface profiles.

Close examination of Table III indicates that there is not much difference in the correlation coefficient, R^2, between Equations 5 and 6, and that these relations give a better fit than either Equations 3 or 4. But from these data alone, it is not possible to know with certainty which of the functions actually fits the best. When all the composites are considered, Equation 6 results in the largest correlation coefficients; thus it is assumed that this function best describes these fracture surfaces. Two typical fits of the data using Equation 6 are shown in Fig. 3. The slopes of the lines are somewhat different between the two materials shown, which may be significant, and will be discussed later. Fits of Equation 6 to the data for all the composites were excellent. This equation will be used further in the form

$$R_S = R_S(0)\eta^p \quad (6)$$

As indicated in the previous section, all profiles were taken from 200× photographs. What would the

TABLE II Measured surface roughness parameter, R_S

Alloy No.*	η (μm)									
	2.1	4.2	8.3	12.5	18.8	23.0	29.2	37.6	43.9	48.1
6	1.87	1.72	1.55	1.40	1.21	1.10	1.11	1.07	1.05	1.05
4	2.00	1.65	1.33	1.22	1.09	1.11	1.00	0.955	0.926	0.909
8	1.96	1.82	1.61	1.52	1.32	1.27	1.14	1.16	0.965	1.01
12	1.53	1.36	1.23	1.17	1.09	1.06	1.02	0.974	0.969	0.964

*Alloy 6 = 2014 + 15 vol % SiC PA (see Table V); Alloy 4 = IN-9021 + 14 vol % SiC PA; Alloy 7 = 2014 + 25 vol % SiC PA; Alloy 12 = 2024-T351.

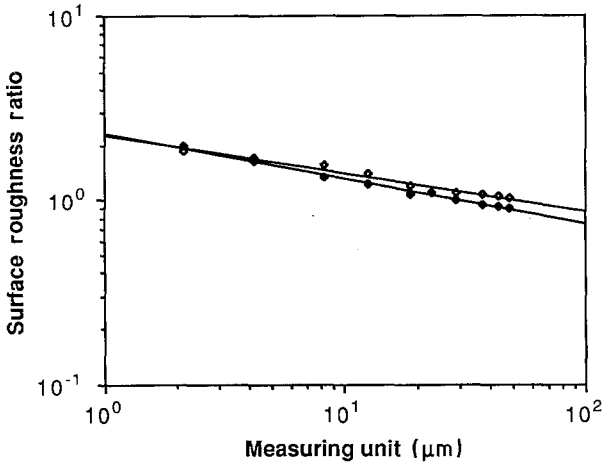

Figure 3 Surface roughness ratio parameters as a function of the measuring unit for two of the composites, showing the similarity in magnitude of R_S and the linearity of the relationship when plotted this way. (◇) Alloy 6, (◆) Alloy 4.

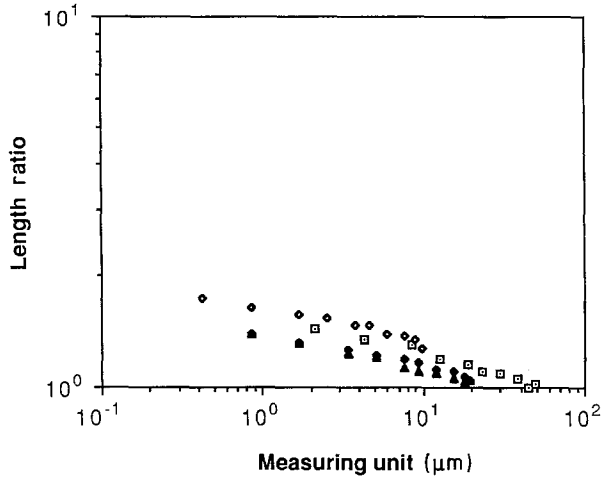

Figure 4 Comparison of profile length ratio parameters measured at different photographic magnifications for 2024-T351 fracture surface. Magnification (□) 200 ×; (◆, ▲) 500 ×; (◇) 1000 ×.

effect be if a smaller measuring unit were used? For insight into this issue, photographs of 2024-T351 were taken at 500 and 1000 × and analysed. Values for profile and surface roughness parameters at all magnifications are given in Table IV, as are values of the profile and surface fractals, D_L and D_S. The variation of R_L with η is shown in Fig. 4, where good agreement may be seen for results between the two 500 × photographs and between the 200 × and the 100 × photograph. Similar results were obtained for R_S. It is concluded that decreasing the value of η from 2.12 (200 ×) to 0.42 μm (1000 ×) had no effect on the description of this fracture surface.

3.2. Fracture toughness

Values of fracture toughness determined using the procedures outlined previously are given in Table V, together with measured roughness parameters. Duplicate tests were conducted for most of the composites, with reasonable agreement between measured values. Alloy 12 was available in the laboratory, and it was tested to compare with Alloy 11, both in fracture surface roughness and toughness and for comparison of the fractography of these materials. However, a low value of fracture toughness was measured, compared with values known for this material, so a second specimen of 2024 was obtained from a plate of material (Alloy 13 of Table V) obtained from another investigator in our laboratory who had used different loading equipment and had measured the crack length optically. The value he determined, shown in brackets, compares very well with the value measured using the computer-controlled equipment. Thus, it is concluded that fracture toughness values determined using the computer-controlled equipment are reasonably accurate.

The fracture roughness parameters $R_S(0)$ given in Table V are compared to the toughness values in Fig. 5. It is appropriate to compare R_S with toughness because it is indicative of the actual surface area of the specimen. There is no discernible correlation between these two material characteristics for these composites. Rather, these data could be construed as indicating the presence of an "optimum roughness" of between 2 and 2.5, which seems to have no physical interpretation.

Other investigators have used the fractal dimension for a comparison of toughness values. Fractal dimension may be determined directly from the exponent of the equation for R_L or R_S, when it has the form of Equation 6, through the simple relation

$$D_L = 1 - p \quad \text{or} \quad D_S = 2 - p \qquad (7)$$

The exponent of Equation 6 is also the slope of the lines in Figs 3 and 4.

4. Discussion

4.1. Fractals

To date, only a few tests have been made of the hypothesis that fracture surface topography can be described by a fractal dimension. The initial results of Mandelbrot *et al.* [2] supported the hypothesis, but subsequent work by Pande *et al.* [5] and Underwood and Banerji [3, 4] provides less support. The data in Fig. 3 of Mandelbrot *et al.* [2] should be compared

TABLE III Relationships between R_S and η which were examined*

Alloy No.	Equation 3, $R_S = a + b\eta$			Equation 4, $R_S = ae^{b\eta}$			Equation 5, $R_S = a + b\ln\eta$			Equation 6, $R_S = a\eta^b$		
	a	b	R^2	a	b	R^2	a	b	R^2	a	b	R^2
6	1.69	−0.0163	0.788	1.69	−0.0120	0.826	2.10	−0.285	0.973	2.226	−0.204	0.981
4	1.61	−0.0183	0.719	1.63	−0.0142	0.809	2.14	−0.333	0.966	2.34	−0.248	1.00
7	1.82	−0.0194	0.895	1.85	−0.014	0.935	2.26	−0.320	0.979	2.48	−0.224	0.948
12	1.37	−0.0101	0.790	1.37	−0.0087	0.838	1.63	−0.179	0.991	1.69	−0.149	1.00

* R^2 = correlation coefficient.

TABLE IV Effect of measurement dimension*

Photograph Magnification	$R_L(0)$	p	D_L	R^2	$R_S(0)$	q	D_S	R^2
200 ×	1.60	−0.115	1.12	0.978	1.78	−0.140	2.14	0.975
500 ×	1.39	−0.087	1.09	0.966	1.50	−0.106	2.11	0.963
500 ×	1.38	−0.096	1.01	0.992	1.49	−0.117	2.12	0.992
1000 ×	1.63	−0.086	1.09	0.943	1.80	−0.100	2.10	0.940
All mags	1.515	−0.106	1.11	0.860	1.65	−0.128	2.13	0.860

*$R_L = R_L(0)\eta^p$; $R_S = R_S(0)\eta^q$; $D_L = 1 - p$; $D_S = 2 - q$.

with that of Fig. 2 of Pande *et al.* [5] and Fig. 10 of Underwood and Banerji [3]. The hypothesis may be tested by determining how well Equation 6 fits the data. Or, how well does a straight line fit the data when $\log R_L$ is plotted against $\log\eta$? For the results of Underwood and Banerji there is curvature for both small and large η, but their data show that for $4 < \eta < 50\,\mu$m the fit is reasonably linear. Pande *et al.* [5] achieve a good fit for three of their six curves over the range $4 < \eta < 148\,\mu$m with little non-linearity seen for large and small η.

The results of Figs 3 and 4 indicate the data are fitted reasonably well by Equation 6 over the range of η for which measurements were made, $2.12 < \eta < 48.1\,\mu$m. Even the one case where much smaller values of η were investigated showed a good fit. Thus, the results of this investigation indicate that a fractal dimension does describe fracture surface profiles of these SiC reinforced composites, and unreinforced 2024-T351.

The physical meaning of this result is that these fracture surfaces are self-similar at all the levels of measurement used, so that measurement dimension is not a critical factor in their description.

4.2. Fracture toughness

However, in the context of the present study, the more important question is whether roughness of the fracture surface or the actual surface area correlates with the fracture toughness. In Fig. 5, $R_S(0)$, the surface roughness ratio coefficient, is plotted against the fracture toughness. There is no obvious correlation. A similar result was found for K_C plotted against R_L, the profile roughness factor coefficient. These coefficients were used to represent the surface roughness for a common unit of measurement. They are the values of Equation 6 for $\eta = 1$ and do not represent actual values of profile or surface roughness.

The concept of a relation between fracture toughness and the fractal dimension, D_L, is examined in Fig. 6. A similar result was obtained by plotting K_C against D_S. As with profile and surface roughness factor coefficients, there is no correlation between fracture toughness and fractal dimension.

The reasons for this lack of correlation between fracture toughness and any descriptor of fracture surface roughness is that fracture toughness for the materials examined here is mainly related to the work done within the plastic zone of the crack as it grows through the material. Work is also expended by the increase in surface area as the crack extends. The growth of a void sheet during final fracture would be a particularly work-intensive form of crack passage, but fractography of this material shows only a limited number of small dimples. Examples of fractography are shown in Fig. 7. Although these surfaces are rough, very little work was expended in their actual formation, as compared to the work dissipated by plastic deformation within the plastic zone. These concepts have been demonstrated for Alloy 1, which has the smallest of the measured fracture toughnesses [6], and is being examined for Alloy 6, which has the

TABLE V Fracture toughness and roughness

Alloy No.	Designation	Condition*	Toughness, K_c (MPa m$^{1/2}$)	Roughness, R_S	D_S
1	IN-9052 + 15 vol %	AR	8.7, 9.1	1.3	1.084
2	Al-4Mg + 15 vol %	AR	12.2, 12.2	2.1	1.170
3	IN-9021 + 14 vol %	AR	13.4	1.6	1.106
4	IN-9021 + 14 vol %	PA	13.8	2.3	1.248
5	2014 + 15 vol %	AR	13.8, 14.3	1.6	1.119
6	2014 + 15 vol %	PA	20.0, 22.6	2.3	1.204
7	2014 + 25 vol %	AR	14.3, 15.4	2.5	1.224
8	2014 + 25 vol %	PA	11.7, 13.9	2.8	1.216
9	7475 + 15 vol %	AR	13.4, 13.7	3.8	1.269
10	7475 + 15 vol %	PA	13.0, 16.0	2.4	1.207
11	2024 + 15 vol %	PA	14.7, 17.7	2.4	1.205
12†	2024-T351	PA	21	1.7	1.149
13†	2024-T351	PA	36 [33]	1.8	1.140

*AR = alloys received as extruded bars of rectangular cross-section and not further heat-treated; PA = heat-treated according to the recommendation of the manufacturer to obtain conditions equivalent to peak strength (−T6) in the matrix.
†Alloys taken from different plates, both manufactured and peak-aged by Alcoa.

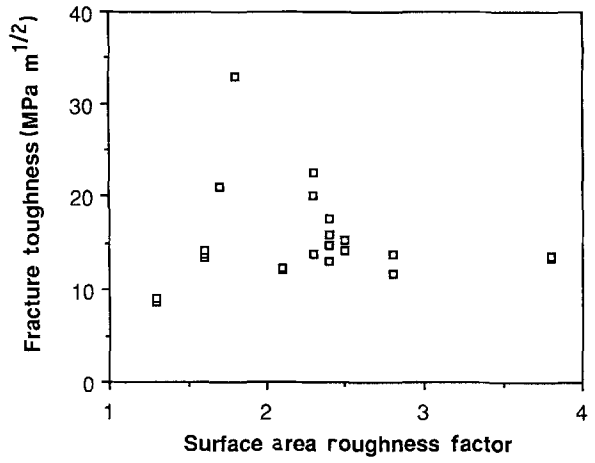

Figure 5 Comparison of fracture toughness and surface roughness ratio for all the composites tested.

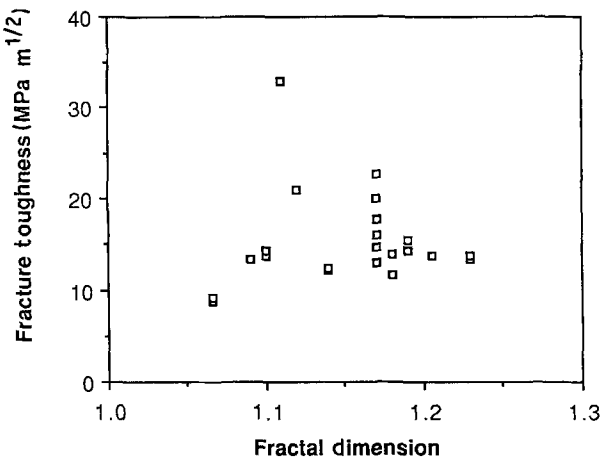

Figure 6 Comparison of fracture toughness and fractal dimension derived from the profile length ratio R_L for all the composites tested.

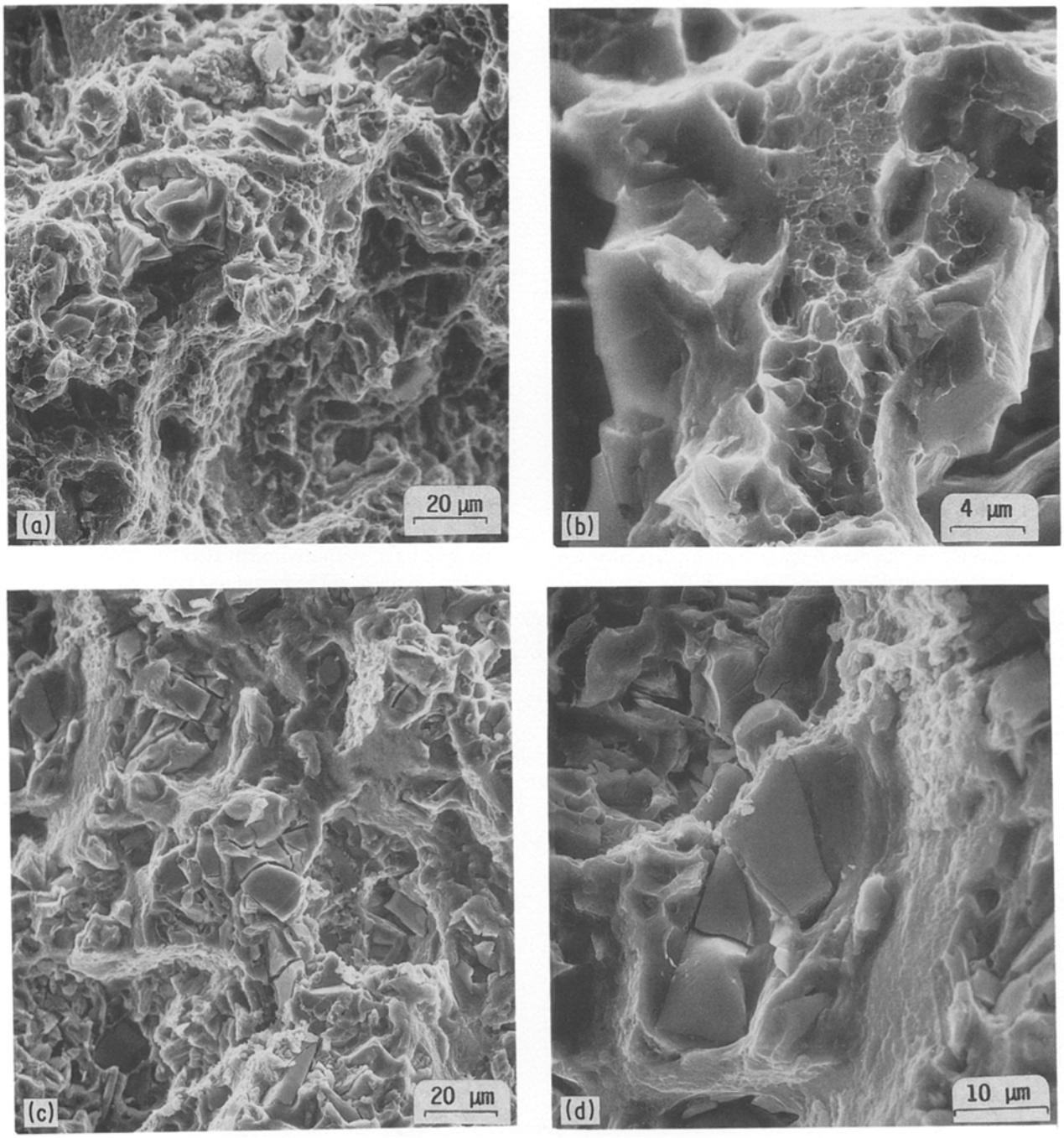

Figure 7 Fractography of two of the composites tested, showing some regions of dimples which are both small in size and cover only limited regions of the surface. All photographs are of 2014 + 15 vol % SiC. (a) and (b) are from as-received material; (c) and (d) are from peak-aged material. Direction of crack growth was from left to right.

largest K_c. Three factors control the amount of work expended within the plastic zone per unit area of crack growth: (i) the size of the plastic zone, (ii) the strain which the material can sustain at the crack tip, and (iii) the magnitude and shape of the stress–strain curve.

The discussion above may also apply to other materials, but as the size and number of dimples caused by microvoid growth and coalescence increases, so will the work done in their formation. The expenditure of work in forming the void sheet will begin to rival the work done within the plastic zone at some point, and must be considered. The presence of large dimples will increase the fracture surface roughness, so it is more likely that a fracture surface roughness parameter would correlate with fracture toughness for materials exhibiting very ductile fractures.

From Equation 6, it is not possible to determine the actual surface area because as η approaches zero the magnitude of R_S becomes unbounded. If some curvature had been found in the measurement of R_S at small η, then the data could have been fitted to an equation of the form

$$R_S = R_S(0)(\eta + \eta_0)^d \quad (8)$$

which does converge to $R_S(0)(\eta_0)^d$ for $\eta = 0$. This same functional form has been used to describe the strain distribution within the plastic zone of fatigue cracks [7]. Unfortunately, the constants in Equation 8 cannot be determined from the measurements of surface roughness thus far made for these alloys. Therefore, the actual surface area cannot be obtained, only estimated.

5. Summary and conclusions

1. Fracture toughness was measured for a series of silicon carbide reinforced aluminium alloy composites.

2. Profile and surface roughness ratios were measured from the fast fracture zones of these composites. These ratios were described well by a fractal dimension, meaning that the roughness of these fracture surfaces were self-similar when measured over the size range of 0.48 to 48 μm.

3. Fracture toughness did not correlate with either the fractal dimension or the profile or the surface roughness parameter coefficient, which is contrary to the analysis of previous investigators. An explanation is offered for this finding.

Acknowledgements

This work was performed as a part of research on the fracture characteristics of composites by the Office of Naval Research, Contract N0014-85-C-0206, contract monitor Dr S. Fishman. Fracture toughness and fracture surface profile photographs and measurements were done by Jim Spencer. Dick Sharron wrote the software used by the image processing equipment for roughness measurements. Professor Underwood and Dr Pande supplied some of the references from which ideas came. The author is grateful for the skilled and enthusiastic help and support of all these persons.

References

1. E. E. UNDERWOOD and K. BANERJI, "Metals Handbook", Vol. 12 (ASM International, Metals, Park, Ohio, 1987) pp. 193–210.
2. B. B. MANDELBROT, D. E. PASSOJA and A. J. PAULLAY, *Nature* **308** (1984) 721.
3. E. E. UNDERWOOD and K. BANERJI, *Mater. Sci. Engng* **80** (1986) 1.
4. *Idem*, "Metals Handbook", Vol. 12 (ASM International, Metals Park, Ohio, 1987) pp. 211–215.
5. C. S. PANDE, L. R. RICHARDS and S. SMITH, *J. Mater. Sci. Lett.* **6** (1987) 295.
6. D. L. DAVIDSON, *Metall. Trans. A.* **18A** (1987) 2115–2128.
7. *Idem, Engng Fract. Mech.* **25** (1986) 123.

Received 15 December 1987
and accepted 4 May 1988